System Considerations of an Image Assisted Total Station – Evaluation and Assessment

Systembetrachtungen einer bildgestützten Totalstation – Evaluierung und Einordnung

Alexander Reiterer, Andreas Wagner

To close the gap between existing low-resolution, medium-accuracy sensors and conventional (co-operative target-based) surveying systems, Image Assisted Total Stations are a promising solution. The combination of image-based measurement methods with a motorized total station enables the development of a highly accurate and fully-automated point detection system. The study at hand evaluates this new multi-sensor system with regard to the image components. The evaluation includes a comparison of different image-based measurement methods, an investigation regarding the precision, an assessment of target/object size and rotation, and a long-time stability test. An estimation of the potential of Image Assisted Total Stations for the future completes this study resulting in a broad overview of these new measurement systems.

Keywords: Image Assisted Total Station, Image Point Detection, Edge Detection, Template Matching.

Bildgestützte Tachymeter stellen eine vielversprechende Neuentwicklung dar, um die Lücke zwischen niedrig auflösenden Systemen mittlerer Genauigkeit und konventionellen Messsystemen (basierend auf kooperativen Zielpunkten) zu schließen. Die Kombination von Bildmessmethoden und motorisiertem Tachymeter ermöglicht die Entwicklung von hoch genauen und voll automatisierten Punkterfassungssystemen. Der vorliegende Beitrag präsentiert eine Evaluierung dieser neuen Messsysteme, unter dem speziellen Gesichtspunkt der bildgebenden Sensorik. Die Untersuchung inkludiert einen Vergleich unterschiedlicher Bildmessmethoden, Tests hinsichtlich der Präzision, Versuche betreffend der Größe und Rotation von Zielobjekten, und einen Langzeittest. Eine Abschätzung des zukünftigen Potenzials bildgestützter Tachymeter komplettiert die Publikation, welche dem Leser einen breiten Überblick über diese neuen Messsysteme gibt.

Schlüsselwörter: Bildgestützte Totalstation, Bildpunktdetektion, Kantendetektion, Mustererkennung

1 INTRODUCTION:

Image Assisted Total Stations (IATS) represent a new kind of tacheometers. They offer the user (metrology expert) an image capturing system (CCD/CMOS camera) in addition to a polar 3D point measurement system. The system is capable of capturing panoramic image mosaics through camera rotation – with appropriate calibration, these images are accurately geo-referenced and oriented, and can be immediately used for direction measurements with no need for object control points or further photogrammetric orientation processes.

The development of IATS has to be seen in combination with research work done in the field of reflectorless distance measurement systems (e.g. Gottwald 1987, Katowski 1989). The latest developments in the area of IATS are done by Leica Geosystems (Walser 2004, Leica Geosystems 2011), the Ruhr-Universität Bochum (Scherer

2004), the i-MeaS project at Vienna University of Technology (Reiterer et al. 2010), the alpEWAS project at the Technische Universität München (Wasmeier 2009), Topcon (Topcon 2011), and Trimble (Trimble 2011).

Some previous evaluations on precision and potential of these new measurement systems can be found in Walser (2004), Reiterer (2004), and Wasmeier (2009). The aim of the work at hand is to evaluate three object detection methods for IATS and to analyse the potential for future applications.

The paper is divided into two main parts: The first part (Section 2) gives an overview about the system design of an IATS and image-based measurement techniques. The second part (Sections 3 and 4) presents an evaluation of the used image-based measurement techniques in combination with the IATS and an assessment of the potential of this combination. A conclusion (Section 5) completes the paper.

2 IMAGE-BASED TACHEOMETRY

2.1 The Measurement System (Image Assisted Total Station)

The present study is using a IATS prototype (Figure 1) which is based on a total station (Leica Geosystem TPS 1201) with a colour CMOS camera (½ inch, 2560 × 1920 pixel, with a pixel size of 2.2 × 2.2 µm) in the optical path (for this camera set-up the focal length is 228.5 mm resulting in a field-of-view of 1.56 × 1.17 gon). One pixel on the image sensor corresponds to an angular value of 0.61 mgon. The maximum frame rate (MFR) depends on the selected resolution of the image. By adapting the image size MFR can be increased, e.g. capturing full-frame images results in a MFR of 5 Hz, whereas an image size of 144 × 144 pixel leads to a MFR of 200 Hz.

In literature (Walser 2004, Wasmeier 2009) two different approaches exist for calibrating an IATS, both using the theodolite axes correction terms, vertical-index, collimation and tilting-axis errors to define the theodolite pointing axis. Comparing the two approaches has shown that the results are significantly equal. The advantage of the approach of Wasmeier (2009) lies in the calculation of the focal length within the calibration process – Walser (2004) requires prior knowledge about the optical system. A calibrated system allows for the expression of the measured pixel position on the image sensor as field angle in the object space. The mathematical derivation can be found in literature and will not be exposed at this point.

At the Technische Universität München (Chair of Geodesy) three structural identical IATS are currently available. Therefore, some of the in Section 3 presented tests are using this fact and are comparing the results of all three measurement systems.

2.2 Image-Based Measurement Procedures

Using an IATS the procedure of point/object identification can be extended to a template- and/or edge-based measurement process. In the following we will present three different techniques for object measurement: edge-based, template-based, and point-based method. At the moment these methods are working separately – the user has to decide which method should be used and how (e.g. parameter setting, etc.). A suitbale algorithm has to be selected on the basis of the specific application. Possible questions to choose a method are, e.g. *Which kind of points/features are representing the object? Which precision is necessary for feature detection and following up 3D measurement? Is a real-time application necessary?* At the end of this study (Section 4) we will present a **decision matrix**, which can be used to select a suitable detection algorithm for specific applications.

Edge-Based Measurement Method: Edge detection is one of the essential tasks in computer vision. An enormous number of different algorithms can be found in the literature (as shown in Shapiro & Stockman 2001) – well known and commonly used are the *Canny*, the *Sobel* and the *Prewitt* operator. The present work is based on a modified implementation of the Canny algorithm (Canny 1986, Lanser & Eckstein 1992).

The used edge extraction is performed to a region-of-interest (ROI) which contains the target. This pre-selection has two main advantages: (1) by restricting the process to a ROI the relevant edges can be easily selected, and (2) a reduced domain is an efficient way to speed-up the process. The main goal is to select automatically the relevant contours and to extract the lines within the ROI. For representing a High Definition Survey (HDS) target (as used in our tests – see Section 3) all detected contours are divided into line and arc segments, whereas the last ones are deleted. Additional short arcs, which are recognized as lines have to be omitted for further processing. All remaining collinear contours are approximated to a (straight)

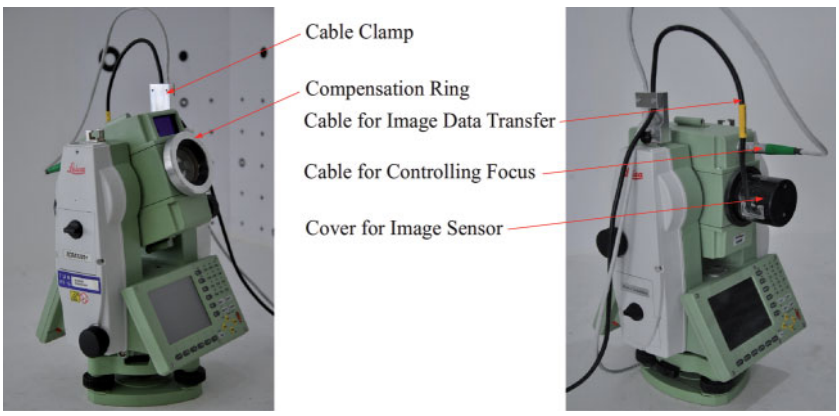

Fig. 1 | Prototype of an Image Assisted Total Station

line by weighted least square fitting. To reduce outliers in the fitting procedure the approach of Mosteller & Tukey (1977) is used, where the dependent variables are weighted by a function of the residuals.

For all test series the same evaluation parameters have been used, such as the size of the edge detection filter or minimum length of a detected line. However, automated selection, classification and segmentation of the detected lines is a crucial task and can processed by means of high programming effort and long learning phases only[1].

Advantages of the edge-based approach are the high precision and reliability of feature detection, the real-time capability, and the availability of a huge number of different detection algorithms and implementations. The disadvantages are the sensitivity to changes of the light situation, and the required user interaction for the selection of necessary parameter.

Template-Based Measurement Method: Template matching enables to find and localize objects based on a pattern, which is presented in a training image. A common recognition technique is to find the maximum correlation between two functions (template and search image) based on grey values. Unfortunately correlation-based matching is unreliable when objects are scaled or rotated, or illumination is changed. This disadvantage can be eliminated by extracting features along contours and using them for matching, which leads to the approach of shape-based matching.

For our approach each template pixel as well as each pixel of the search space is associated with the direction vector by (identical) edge filtering. The similarity measure is the sum of the dot product of these vectors over all points of the model. In this way the algorithm is robust to occlusion and clutter, because missing parts or fragments in the search image will result in a zero-sum or mostly in small values. The result of that product is a score between 0 and 1, whereas the latter indicates a perfect match.

To speed up the matching process an image pyramid (both for the model and the search space image) is created, consisting of the original, full-sized image and a set of down-sampled images (the number of levels has to be chosen depending on the complexity of image and template – in our study 7 levels represent the best compromise between reliability and computation time). The actual search is performed for the top level pyramid and the similarity measures are computed for all model variations. A potential correspond is defined by a larger score as an user-defined threshold and a local-maximum with respect to neighbouring scores. After having recognized such a potential match it is tracked through the resolution hierarchy until it is found at the lowest pyramid level. This process

[1] Examples for parameters which have to be specified by the user, are the (upper and lower) thresholds for the hysteresis. Points with an amplitude (second derivative) larger than the upper threshold are immediately accepted as belonging to an edge, while points with an amplitude smaller than the lower threshold are rejected. The selection of the thresholds is correlated with the amplitude and width of the line as well as the choice of the filter width (for our examples the upper threshold has been determined on the basis of the minimum plus the half range of the grey values of the image, the lower threshold has been fixed to 1).

results in the parameters of the affine transformation for the (centre of gravity of the) model: translation, rotation and scale.

To achieve highest precision several approaches are used: (1) the extracted model points as well as the feature points in the image are calculated with sub-pixel accuracy, (2) a polynomial fit to the similarity measurement values in the neighbourhood around the maximum score is applied, and (3) a least square adjustment minimizes the sum of squared distances for each model and image point, whereas additional information from the direction vectors is used. Steger (2000, 2002) formulates a precision of 1/22 pixel and 1/100 degree for this approach.

Advantages of the template-based approach are the capability to fully automate the detection process, the real-time capability, and the possibility to design the process as an user-driven procedure (user has the possibility to select a template directly in the search image). The disadvantage is the sensitivity to changes of the light situation.

Point-Based Measurement Method: In the literature a huge number of different methods for image point detection exists (Harris & Stephens 1988, Förstner & Gülch 1987, Smith & Brady 1997, Marr & Hildreth 1980, Lowe 2004, Rosten & Drummond 2005, 2006). As a measurement system has to be able to capture object points in (nearly) real time, we are using a point detection method on the basis of the *determinant of the Hessian* (Bay et al. 2008). This method works with second order Gaussian derivations and delivers interest points in blob-like structures directly. An implementation working on this principles is SURF (Bay et al. 2008), which was developed originally at the ETH-Zurich (the acronym stands for „Speeded Up Robust Features"). This algorithm uses an approach similar to the well-known SIFT operator (Lowe 2004) with a special focus on reduced computation time.

Reiterer et al. (2010) were the first to implement the SURF algorithm for an Image Assisted Total Station. They used the measurement procedure for deformation monitoring of natural objects – the work at hand is based on this implementation and parameter setting. In the present study 10 image points are detected for each image (this number is a compromise between resulting precision and processing time). These image points are averaged to one point which describes the actual image/target.

Advantages of the point-based approach (SURF) are the capability to fully automate the detection process, the possibility to use the result for 3D-point detection/measurement directly (using spatial intersection by two IATS), and the availability of run-time optimized implementations. The disadvantages are the sensitivity to changes of the light situation, and the computational complexity (not fully real-time capable).

3 EVALUATION OF IMAGE-BASED MEASUREMENT METHODS

Measurement precision and reliability depend on the measurement sensor (hardware), measurement methods and calculation methods (software). As the hardware of such a system is based on a conventional total station, we will focus our study on the components which are integrated additionally: image sensor and image-based data acquisition methods. Due to the fact that the separation of these two components is not possible (for most tests), we will pool these parts as *imaging system*. Several studies (Stempfhuber & Wunderlich 2004, Juretzko 2006) have confirmed the high precision of the basic sensor (Leica Geosystems TPS 1201) given by the manufacturer (angle measurement standard deviation of 0.3 mgon, reflectorless distance measurement accuracy of ± 2 mm ± 2 ppm).

Because image-based measurements are highly depending on the configuration of the imaging system (e.g. position of the focus lens) the tests are performed by means of one (fixed) configuration. For most tests (expected the test concerning daylight/artificial light, and resolution) the whole measurement setting was based in a climatic chamber (7×2 m) to ensure constant temperature and light situation. Furthermore, for all tests (expected long-time stability test) a warm-up phase of 3 hours has been taken into account (warm-up of the measurement system at ambient temperature and with connected power supply). The IATS was mounted on a grounded measurement pillar, the target (resp. target sheet) was fixed on the wall of the chamber. Distance between the measurement system and the target was 6.08 m. As target a compilation of different signs (including edges, a HDS target, and a structured area) was used (see Figure 2). As the used image processing techniques achieve their highest precision on the basis of black-and-white images, we have used grey level instead of colour information.

All subsequent tests have been performed repetitively by capturing image. The first image of each series has been defined as reference – differences (Δ) are calculated between actual image and reference. The stated standard deviations (σ) are based on these differences – uncertainties of the standard deviations have been calculated as described in BIPM (GUM) (2008). It should be noted that the presented data have been captured under laboratory conditions for well selected measurement configurations. To have robust results each scenario has been repeated at least three times.

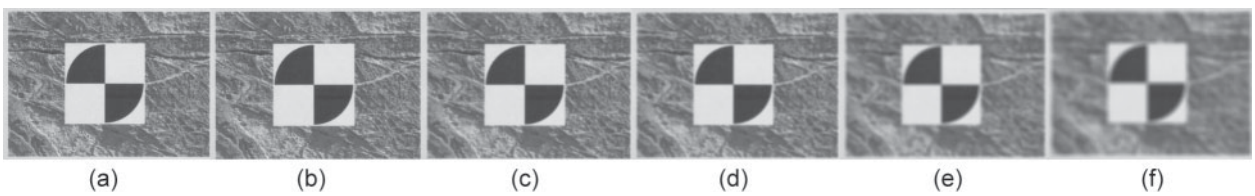

Fig. 2 | Template captured by different focus positions (a=focus position 1 – f=focus position 6)

	IATS 1		IATS 2		IATS 3		Mean Values	
	σ_y	σ_x	σ_x	σ_y	σ_x	σ_y	σ_x	σ_y
Edge-Based	0.03	0.04	0.03	0.04	0.04	0.04	**0.03**	**0.04**
Template-Based	0.06	0.06	0.07	0.06	0.08	0.07	**0.07**	**0.06**
Point-Based	0.10	0.06	0.11	0.06	0.08	0.06	**0.10**	**0.06**

Tab. 1 | Standard deviations [pixel] for edge-based, template-based, and point-based method for the three used IATS (uncertainty of $\pm 0.04 \cdot \sigma$)

3.1 Precision

The *precision* (sometimes also referred to as "internal accuracy") of an image-based system has been defined by Wolf (1966) as a measure of quality depending on repetitive captured images and subsequent processing steps only. Standard deviation describing the precision is depending on image capturing, data transfer from image sensor to the processing unit, and image processing algorithms. The following tests have been processed on short distances (6.08 m) capturing images in short time intervals (3 Hz). They present the most representative data sets and figures of different time series which have captured under comparable conditions. The relevant factors describing the precision of our measurement system are the object detection algorithms, their precision, the signal-to-noise-ratio of the image sensor and the resolution of the imaging system.

(a) Precision of Object Detection Algorithms

The following tests are based on the configuration as described at the beginning of this section. The target has been captured by 300 images. As shown in Table 1, the evaluation on basis of the different measurement devices does not show significant differences. Due to technical reasons, the measurements could not be performed simultaneously. Thus slight variations may be explained by changed conditions, e.g. airflow. Comparing the different algorithms the edge-based method shows the highest precision, with standard deviations between 0.03 and 0.04 pixel in x- and y-direction (which corresponds to 0.02 mgon). The precision of the other two methods (template- and point-based) differ by factor 2 ($\sigma = 0.06$ to 0.10 pixels, resp. 0.04 to 0.06 mgon). Points detected by the SURF algorithm include some outliers which partly increases the standard deviation up to 0.11 pixel (0.07 mgon) and are therefore an explanation for the lower precision. Uncertainty for the standard deviations is $\pm 0.04 \cdot \sigma$.

In an additional test the behaviour of the image-based measurement methods with regard to *defocused images* has been investigated. The configuration of the test setting has been unchanged – focus lens position has been moved by the control software in hundred steps ($\Delta_{focus} = 100$ steps) starting from lens position 5390 (which corresponds to a distance of 6.08 m) with a well-focused image (see Figure 2a) and ending at 5890 (which corresponds to a distance of 5.43 m) with a totally blurred image (see Figure 2f). The first image captured has been defined as reference image. It should be noted that the focus lens can be moved by 18000 steps – focus position 0 corresponds to the maximum object distance (∞), focus position 18000 to the minimum object distance (1.6 m).

Figure 3 shows that the detection methods react differently to defocusing. The edge-based method is almost robust against defocusing – even in the last measured focus position (Figure 2f) the standard deviation is in the range of 1/10 pixel ($\sigma_x = 0.10$ and $\sigma_y = 0.08$ pixel, resp. 0.06 and 0.05 mgon). In contrast, the results of the template-based method are significantly deteriorating starting from focus position 4, as well as for the point-based method. While template matching still achieves a standard deviation of $\sigma_x = 0.37$ and $\sigma_y = 0.62$ pixel (resp. 0.23 and 0.38 mgon) for the last focus position, point detection and subsequent point matching fails. Each focus position has been represented by 10 images, which leads to an uncertainty of the standard deviations of $\pm 0.24 \cdot \sigma$.

The test has shown that the used image processing techniques offer different behaviour concerning unfocussing/blurring. Whereas the edge-based method is nearly invariant on this issue, with only slightly decreasing precision, the other methods need a relatively well-focused image (± 300 focus steps for a distance of ~ 6 m).

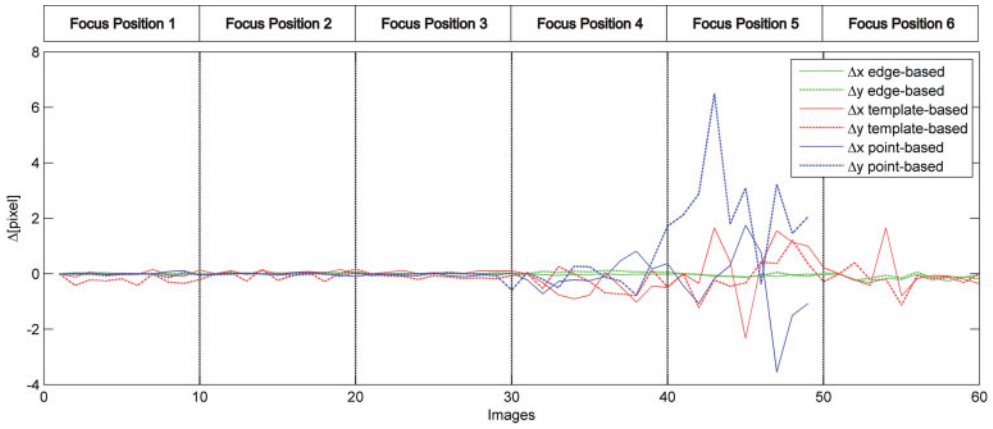

Fig. 3 | Effect of a defocused image onto edge-based, template-based, and point-based method – differences related to a reference (first image of focus position 1)

Comparing the *processing time* of the three detection algorithms leads to 0.5 second for edge-based, 0.2 second for template-based, and 5 second for point-based method (it should be noted that processing time depends on the number of extracted features). Performance can be improved by using special implementation techniques, such as using the graphical processing unit (GPU) and/or using parallel central processing units (CPU) to extract distinctive features from an image. As a consequence of the runtime behavior edge-based and template-based method can be described as fully real-time capable, point-based method as nearly real-time capable. This fact can be useful for the selection of a suitable algorithm for performance critical applications.

(b) Signal-to-Noise-Ratio (SNR)

The signal-to-noise-ratio (SNR) is used to characterize the quality of signal detection of a measuring system. For an image-based measurement system the SNR is given by the ratio of the light signal to the sum of the noise signals. It is expressed as a ratio or factor in units of decibels [dB]:

$$SNR = 20 \cdot \log\left(\frac{g}{\sigma_n(g)}\right) \quad [dB], \tag{1}$$

where g is the mean of the grey levels and $\sigma n(g)$ the corresponding standard deviation. Noise not only changes depending on exposure setting and camera model, but it can also vary within an individual image (characteristics of the captured scene). Therefore it is important to evaluate the SNR for different grey tones.

For measuring and evaluating SNR a target consisting of five different areas each filled by a specified grey tone has been captured under two different lighting situations – (1) using an illumination of 25 lx representing ideal laboratory light conditions, (2) using an illumination of 200 lx representing a slightly overexposed situation. For the test stable lighting is of fundamental importance and is ensured by performing the test as described at the beginning of Section 3. Table 2 shows SNR for the five grey tones (10 %, 20 %, 40 %, 60 %, and 70 %).

It should be noted how noise becomes less pronounced as the tones become darker. Brighter regions have a stronger signal due to more light, resulting in a higher SNR. Therefore overexposed images will have higher visible noise – even if image brightening is processed afterwards. Calculating mean values for SNR results in 70 and 86 dB, respectively. The first value (for an illumination of 25 lx) can be described as slightly higher than SNR of conventional industrial imagining systems (typical values are between 20 and 60 dB), the latter one (for an illumination of 200 lx) as clearly higher. Both values confirm that IATS should be used preferably under ideal light situations (e.g. well-illuminated objects). Especially over- and under-exposed scenes result in noisy images and may lead to inaccurate object detection. A rigorous analysis of the influence of SNR to the precision of object detection is beyond the scope of this study – a detailed evaluation will be the subject of further research work.

Grey Tone	SNR [dB] 25 lx	200 lx
10%	81	99
20%	71	89
40%	68	87
60%	64	81
70%	64	76

Table 2 | Signal-to-noise-ratio for different grey tones

(c) Resolution of the Imaging System

To test the resolution (the capability to capture and measure two single objects as separated) of IATS an evaluation as published by Wasmeier (2009) has been performed. As the results are equal, we will only summarize them – for a detailed description we refer to the literature.

The evaluation shows that (under laboratory conditions) the resolution of the imaging system combined with sub-pixel object or point detection exceeds the precision of angle measurements (visual aiming) of the total station by a factor of 2-4 – the used total station as basis for the IATS represents the limiting factor. Measuring objects or differences between objects by one single image only without moving the telescope, the system can benefit from the high precision of the imaging system (precision then depends on relative measurements inside the captured image only) – a tenth pixel is possible, which corresponds to 0.06 mgon. Scanning an object by an image bundle leads to the precision of angular measurements of the total station which is as accurate as the basic total station (the used Leica Geosystems total station works with an angle measurement standard deviation of 0.3 mgon).

3.2 Influence of Light Condition

One of the most important preconditions for using an image-based measurement system is the stability of the detection of points and

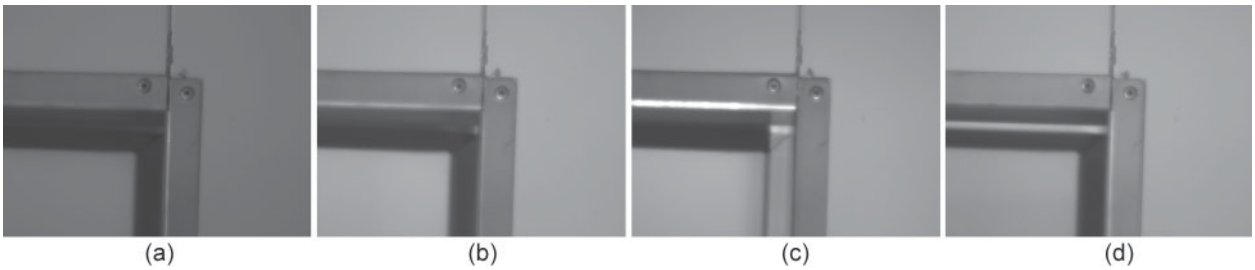

Fig. 4 | Four different light situations for testing – (a) indirect-lighting, (b) direct-lighting coming from left, (c) direct- lighting coming from front, and (d) direct-lighting coming from above

objects under different light conditions. This means that changing the direction and intensity of illumination shall not have any effects on the result. This is an unalterable condition applying the measurement system to objects under uncontrollable lighting situations (variable sun light, luminosity, etc.).

We have captured and measured the corner of a 3D steel construction under different illuminations. Lighting has been varied by moving a 500 W light source around the object – four different scenarios have been simulated (see Figure 4): indirect-lighting, direct-lighting coming from left, direct-lighting coming from front, and direct-lighting coming from above. The illumination causes a considerable effect on the different structures of the objects (e.g. edges are stressed out by varying shadows – cf. Figure 4a and d). Each light situation has been captured by 100 images – measurement set-up has been designed as described at the beginning of Section 3. Calculation of SNR for all images returns values between 64 and 65 dB (constant signal-to-noise-ratio).

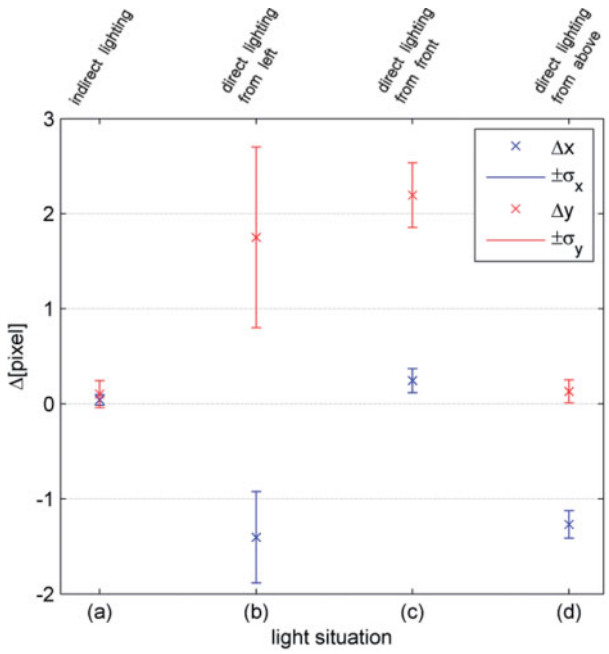

Fig. 5 | Mean values and corresponding standard deviations for the edge-based method (each scene has been represented by 100 images – the first image captured under indirect lighting has been defined as global reference)

For the edge-based method we have chosen the two rivets on the upper part of the steel construction. Each one can be described by a circle with approximately known diameter (depending on shadow) – all following results are based on the left rivet, since both objects showed identical behaviour. Figure 5 shows very impressive the impact of shadow to edge-based method. For the first light situation (indirect lighting), the already identified precision (cf. Section 3.1a) is achieved. In the second scenario (direct light from left), the rivet casts a shadow in the upper right side. The edge-based algorithm detects alternately the (true) edge of the rivet and the edge of the shadow, which results in lower x- and higher y-values – all together the precision rises significantly. With direct light from front, only parts of the circles were detected, caused by the light reflections on the lower part of the metal surface. This leads to a displacement of the y-values (compared with the first light condition). The last scenario (direct light from above) shows the rivet most clearly with nearly no shadow. Detecting the edges results in y-values which correspond to the reference and clearly shifted x-values.

For the template-based method a region just enclosing a rivet has been selected. The results are comparable to those of edge-based method. However, differences can be found in the second and third scenario. While direct lighting from left results in higher, direct lighting from front leads to lower precision. That means, light reflections influence the template-based algorithm, particularly, as in all 400 images the object recognition failed 8 times, mostly in this third lighting scenario. Nevertheless, a recognition rate of 98% was reached which corresponds to Steger (2002).

The point-based method has been applied on the image(s) without image pre-processing or selecting a ROI. The results are comparable to the other two methods – especially, changing the illumination from indirect to a frontal-direct lighting leads to a shifting of detected points around edges, whereas detection on "flat regions" gets results which scattered within the precision formulated in Section 3.1. Furthermore, changing the direction of light results in a huge number of mismatched points. The elimination of such outliers is possible by using RANSAC.

It can be summarised, that the used detection methods are strongly depending on stable light situation. Measuring under natural light can cause considerable problems – image pre-processing techniques (e.g. adaptive histogram equalisation) may help to reduce these influences (Knötzl & Reiterer 2010).

Casott (1999) has worked out that image-based measurement systems are depending on the *type of light* which is used for illuminating the scene. This is emphasized by several publications from Computer Vision and Image Processing (e.g. Nakamura (2006)) describing the selection of suitable illumination as a crucial element in determining the quality of the captured images. To test the influence of different light sources we have processed measurements under artificial light (fluorescent tubes) and under natural light (sun light). The results show no influence of the used light source. A possible explanation of this phenomenon could be the relatively low measurement frequency. Increasing MFR up to 50 Hz results in similar standard deviations. Measuring with a frequency of 200 Hz (artificial light sources as fluorescent tubes are working with ∼100 Hz) requires a significant reduction of image size (see Section 2.1) resulting in a decreased precision – corresponding standard deviations are therefore not comparable.

3.3 Influence of Target Size

Targets with the dimensions of 290 × 233 pixel (target 1), 578 × 470 pixel (target 2), and 1148 × 931 pixel (target 3) have been captured (distance to the object = 6.08 m, measurement frequency = 3 Hz). Figure 6 demonstrates the quality of the images resulting from the different target sizes. To take the influence of the noise into account, for the extracted targets the SNR has been calculated (see Table 3). It can be noted, that the SNR for all targets is nearly con-

	Target 1 (SNR=63 dB)		Target 2 (SNR=62 dB)		Target 3 (SNR=60 dB)	
	σ_x	σ_y	σ_x	σ_y	σ_x	σ_y
Edge-Based	0.03	0.05	0.03	0.05	0.04	0.04
Template-Based	0.08	0.11	0.07	0.10	0.06	0.07
Point-Based	0.14	0.11	0.10	0.06	0.10	0.06

Tab. 3 | Standard deviations [pixel] for three different target dimensions (uncertainty of $\pm 0.04 \cdot \sigma$)

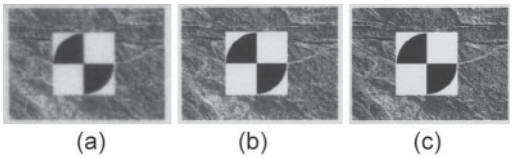

Fig. 6 | Examples of captured targets – (a) 290 × 233 pixel, (b) 578 × 470 pixel, and (c) 1148 × 931 pixel

stant (60-63 dB) – the subsequent evaluated precisions are therefore dependent on the size of the target only. Each target size has been represented by 300 images, which leads to an uncertainty of the standard deviations of $\pm 0.04 \cdot \sigma$.

The results of the edge-based method do not differ significantly for the three chosen resolutions (Table 3). The standard deviations of the x-pixel values scatter from 0.03 to 0.04 pixel (resp. 0.02 mgon), the y-values from 0.04 to 0.05 pixel (resp. 0.02 to 0.03 mgon). The higher standard deviations in the y-direction may be explained by a deflection from the differences at the beginning of the measurement which was measured for all three targets. This abnormality can be found for all three algorithms. For template-based method the standard deviation can be improved by capturing targets with higher resolution, e.g. the values for target 3 ($\sigma_x = 0.06$ and $\sigma_y = 0.07$ pixel, resp. 0.04 mgon) are roughly 25% smaller than for target 1($\sigma_x = 0.08$, $\sigma_y = 0.11$ pixel, resp. 0.05 and 0.07 mgon). The point-based method is also clearly depending on the target size ($\sigma = 0.06 – 0.14$ pixel, resp. 0.04 – 0.09 mgon) – point detection using target 1 shows a reduced precision obviously. Finally we can conclude that a target should have a minimal dimension of 550 × 550 pixel on the image plane for precise measurements.

Comparing the three methods for the detection of targets of different size shows that the edge-based is the most precise under these conditions, with standard deviations between 0.03 and 0.05 pixel (0.02 and 0.03 mgon). In our tests the template-based method reached a precision nearly up to a twentieth pixel. It should be noted, that this applies only to the image with the highest resolution in which the edges were exactly defined and clearly demarcated from the environment. The point-based method provides a precision of a tenth of a pixel and is (nearly) independent of target size. This test has been performed for each of the three different IATS available with the result that no significant differences between the systems concerning the precision of target detection can be revealed.

3.4 Influence of Target Rotation

A target with nine different rotation angles has been captured by 300 images (measurement frequency: 3 Hz). Again, after the capturing process the targets have been extracted from the sheet, resulting in 300 files for each rotation angle – the first target of each series has been defined as reference. The SNR for all targets is between 60 and 63 dB and therefore assumed to be constant. Table 4 show the resulting standard deviations (with an uncertainty of $\pm 0.04 \cdot \sigma$).

It is clearly visible that the three used object detection methods behave differently to rotation of the captured target. Whereas the edge-based method shows no irregularities, the data of template- and point-based methods exhibit divergences for different rotation angles. No statistical irregularities can be found carrying out a Student's t-test with the edge-based method. The template-based method shows significantly higher values for 0° (σ_y), 20° (σ_x,σ_y) and 25° (σ_x) – that means, for this target rotation angles the measurements reach a lower precision than on average. Evaluating point-based method results in significantly lower precision for 25° (σ_x,σ_y) and 35° (σ_y) and significantly higher for 30° (σ_x) and 40° (σ_x) compared to the average. Having analysed the data and repeated the test, no explicit scheme has been identified. Further tests will be necessary to analyse the dependence of the detection algorithm on the rotation of targets more thoroughly.

However, the test shows the relationship of rotated target and rotated reference (same angle) only. The calculation of corresponding objects/points if target and reference have rotated differently has not

		0°	5°	10°	15°	20°	25°	30°	35°	40°
Edge-Based Method	σ_x	0.03	0.03	0.03	0.03	0.03	0.03	0.03	0.03	0.03
	σ_y	0.03	0.03	0.03	0.04	0.03	0.03	0.03	0.03	0.03
Template-Based Method	σ_x	0.08	0.06	0.05	0.04	0.10	0.09	0.04	0.04	0.07
	σ_y	0.10	0.06	0.05	0.08	0.11	0.08	0.06	0.05	0.08
Point-Based Method	σ_x	0.13	0.11	0.15	0.10	0.09	0.18	0.07	0.14	0.06
	σ_y	0.06	0.06	0.05	0.05	0.03	0.08	0.04	0.09	0.04

Tab. 4 | Standard deviations [pixel] of the detection methods (uncertainty of $\pm 0.04 \cdot \sigma$) for targets under different rotation angles

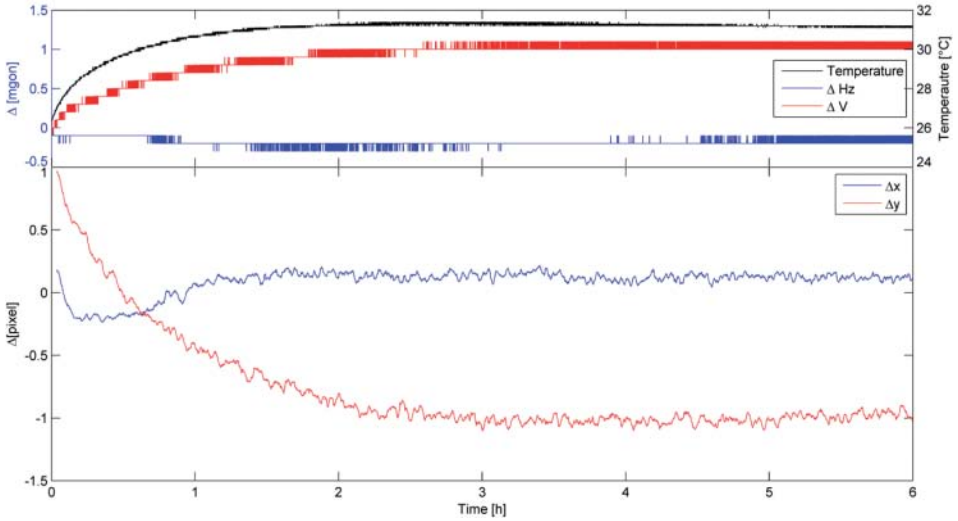

Fig. 7 | Results of the long-time stability test – (top) horizontal and vertical angle, and inner temperature,(bottom) horizontal (Dx) and vertical (Dy) differences detected by edge-based method

been tested yet – a first assessment for point-based detection can be found in Reiterer et al. (2010).

3.5 Long-time Stability

One of the most essential characteristics of measurement systems is their long time stability. Measuring the same target in different time epochs should lead to results which scattered within system's precision only. To test long-time stability and the run-in period a target has been monitored over a period of 36 hours with a measurement frequency of four images per minute. For analysing the data the edge-based method has been used since this detection algorithm is the most precise (see Section 3.1a). Figure 7 shows the first six hours of the test.

As shown in Figure 7 (top) the vertical angle seems to be directly connected to the inner temperature reaching stable values after 3 hours (scattering within the measurement precision), whereas the horizontal angle measurement is stable from the beginning. The bottom graph (Figure 7) shows that image-based measurements are directly connected to the behaviour of the total station resulting in run-in times which are comparable. It should be noted that the vertical component (Δy) needs longer to stabilize.

The thermal stability has already been tested by Wasmeier (2009) with the result that the interior of the total station gets warmed up by 0.7°C due to additional components (e.g. image sensor). This effect has an influence on the horizontal and vertical angle measurement (Hz: 0.1 mgon/°C, V: 0.5 mgon/°C). The warm-up phase as an impact of the additional components lasts for 2 hours.

Summing up, it can be said that the systems has a total run-in time of about 3 hours. Within this run-in time the standard deviation of the detected edges is about 5-9 times higher than the standard deviation of the subsequent measurement period. Capturing data after the run-in time leads to standard deviations as shown in Section 3.1a. As already mentioned above, for all tests a run-in time of 3 hours has been taken into consideration.

4 ASSESSMENT OF THE POTENTIAL OF IMAGE-BASED TACHEOMETRY

In the following the most important facts resulting from the described test are itemized and an assessment of the potential of IATS is formulated. The results can be summarised as follows:

- Template-based and point-based methods are able to measure with a precision of about 0.06-0.09 pixel $\pm$ 0.04·σ (which corresponds to 0.04-0.06 mgon $\pm$ 0.04·σ). The edge-based method is the highest available object detection technique and yields precisions of about 0.03 pixel $\pm$ 0.04·σ (resp. 0.02 mgon $\pm$0.04·σ).
- Long-time tests have shown that the system needs a run-in time of about 3 hours – within this period the precision of detected features is about 5-9 times lower.
- Runtime of the individual algorithms ranges from 0.2 seconds for template matching to a few seconds for the point-based detection method. All three algorithms can be optimized by special implementation techniques (parallelization, using graphical processing unit, etc.) and are therefore suitable for an on-line measurement system with temporal demands.
- The determined precision of all three tested detection methods relates to well focused images. Edge-based detection algorithm seems to be more stable against unfocused/blurred images than point-based or template-based method. An unfocusing of about $\pm$ 300 steps (for a distance of 6 m) has no relevant consequences for all three methods. Note that the relation between focus position and distance is a hyperbolic cotangent function (therefore, an exact positioning of the focus lens has to be considered especially for close-range measurements).
- The average signal-to-noise-ratio of IATS is slightly higher than SNR of industrial imaging systems. This means that IATS should be used under ideal light conditions (well illuminated scenes). The influence of SNR onto the precision of point/object detection methods is still under investigation.
- The used detection methods are only of limited use under varying illumination situations. Further tests and research work to include

image pre-processing techniques (e.g. adaptive histogram equalisation) may help to minimise this problem (Knötzl & Reiterer 2010).

- The system seems to be independent of the dimensions of the used target, but as a requirement for highly accurate target recognition and measurement we can formulate a minimal target size of 550 × 550 pixel.
- The use of template- and edge-based methods is limited in practice (artificial objects can be described by lines and geometrical features, whereas natural objects are rarely characterised by lined structures) – point-based measurement methods are more familiar for geodetic applications and can be used more flexible for describing objects and there surface.

Possible applications are:

- Semi-automated **object reconstruction systems** as described by Walser (2004) and Vicovac (2008). Natural geometric primitives (e.g. corner and edges) can be used to detect descriptive parts of the object. The reconstruction of an object with regular structure could be done by describing and capturing one object element in a learning phase and by detecting and measuring the remaining parts in an automated process (e.g. by *template-based measurement methods*).
- Fully-automated **deformation monitoring systems** as described by Reiterer et al. (2009). The object can be scanned by an image-bundle followed by *point detection*. Using a calibrated multi-sensor system and working with spatial intersection the captured "image point cloud" can be transferred into 3D object space in nearly real-time.
- **Industrial measurement systems** as described by Knoblach (2011). Due to the integrated image sensor IATS can placed without direct access to the eyepiece – targeting can be done by means of a "live-view" manually or automatically. This enables the use of the system under particularly dangerous conditions or in environments which are difficult to access.
- **Measurements of vibration amplitude** could be realised by means of high-frequency image measurements on the basis of IATS. Using the capability of reducing the size of the image matrix and as a consequence thereof the possibility of capturing images with a frame rate of up to 200 Hz (for 144 × 144 pixel) opens new application fields for IATS – the measurement of small vibration amplitudes by abstracting the objects with *edge- or template based methods* could be one (Wasmeier 2009).
- The image sensor enables the capturing of additional information like high-frequency motions or intensity fluctuations of patterns to derive the temperature gradient of atmosphere as decisive influence parameter for **angular refraction effects**. Theoretical foundations regarding such a procedure have been published by Brunner (1979), Hennes (1995) and Eschelbach (2009), practical tests with industrial image-based sensors have been done by Casott (1999), Deussen (2000) and Flach (2000). Currently, a research project at *Technische Universität München (Chair of Geodesy)* explores the suitability of IATS (using *edge detection*) for such applications.
- **Monitoring of cracks** as described by Wasmeier (2009) and Huep (2010). The appearance of cracks on buildings is one of the main problems concerning the stability of artificial structures. Monitoring the changes in crack width is an important diagnostic technique for determining the cause and specifying the remedial work. Using an IATS in combination with *edge- or point-based methods* could help to document, georeference and measure very precisely these phenomenons.

On the basis of the evaluation a **decision matrix** for the three detection methods can be formulated (see Table 5).

5 CONCLUSION

The paper at hand presented the evaluation of an Image Assisted Total Station, a new kind of geodetic sensor for rapid and precise measurements. The tests have shown that with suitable image processing measurements a precision of ~0.05 pixel ± 0.04·σ is possible (which corresponds to 0.03 mgon ± 0.04·σ). These results have to be seen under the consideration that such measurements are image-based only. For measuring in 3D object space the precision of pointing has to be taken into account. Knötzl (2010) has evaluated different IATS system configurations, using polar methods and spatial intersection to measure 3D object points. Polar method results in homogeneous error ellipses, independent of the relative

	Edge-Based Method	Template-Based Method	Point-Based Method
Object Reconstruction	x	x	
Deformation Monitoring			x
High Precision Industrial Applications	x	x	x
Measurements of Vibration Amplitude	x	x	
Angular Refraction Effects	x		
Monitoring of Cracks	x		x
Comments	Actual the most precise detection method, suitable for a large variety of applications, not fully automatable, real-time capable.	Fully automatable method, fully real-time capable, user-driven approach (selection of templates).	Fully automatable method, not fully real-time capable, point-based results can be used for geodetic deformation analysis directly.

Tab. 5 | Decision matrix for the selection of a suitable detection method

position of the observation area, whereas spatial intersection results in error ellipses, which tend to spread along the measurement direction axis (precision of 3D point detection strongly depends on the configuration of the spatial intersection). Note, that polar methods can only be used for distances up to 400 m, because of the limited range of the reflectorless distance measurement.

The study at hand has identified some important facts using Image Assisted Total Stations, e.g. run-in time, long-time stability, dependency from target size and rotation, etc. These facts and the wide experience from practical applications show the high potential of IATS. However, some important influence factors on the precision of the measurements have to be investigated in the future, e.g. SNR, atmospheric effects. The next development step has to be the integration of an Image Assisted Total Station into a general work flow of object monitoring and/or object reconstruction. Furthermore, the automation of IATS measurements will be one of the challenging tasks for the future.

Finally the user (metrology expert, surveyor, etc.) has to decide whether this new measurement system represents a major gain for geodetic work. Total station manufacturers will have to react on the market situation and integrate IATS into their work flow and product line. Commercial systems like Leica's Viva-TS-Series or Trimble's VX using image data for visualisation represent a first step in this direction.

ACKNOWLEDGEMENT:

The research presented in this paper has been supported by the *Alexander von Humboldt Foundation.*

REFERENCES:

Bay, H.; Ess, A., Tuytelaars T.; van Gool, I. (2008): SURF: Speeded Up Robust Features. In: Computer Vision and Image Understanding (CVIU), 2008, Vol. 110, No. 3, pp. 346-359.

BIPM (GUM) (2008): Evaluation of Measurement Data – Guide to the Expression of Uncertainty in Measurement. JCGM 100.

Brunner, F. K. (1979): Vertical Refraction Angle Derived from the Variance of the Angle-Of-Arrival Fluctuations. In: Refractional Influences in Astronomy and Geodesy, Tengström, E. / Teleki, G. (Eds.), pp. 227-238.

Canny, J. (1986): A Computational Approach To Edge Detection. In: IEEE Trans. Pattern Analysis and Machine Intelligence, Vol. 8, No. 6, pp. 679-698.

Casott, N. (1999): Erfassung des Einflusses der „turbulenten Refraktion" auf optische Richtungsmessungen mit CCD-Sensoren. PhD Thesis, Rheinischen Friedrich-Wilhems-Universität Bonn.

Deußen, D. (2000): Meßverfahren zur Erfassung der Vertikalrefraktion unter Nutzung der atmosphärischen Turbulenz. PhD Thesis, Rheinischen Friedrich-Wilhems-Universität Bonn.

Eschelbach, C. (2009): Refraktionskorrekturbestimmung durch Modellierung des Impuls- und Wärmeflusses in der Rauhigkeitsschicht. KIT Scientific Publishing.

Flach, P. (2000): Analysis of Refraction Influences in Geodesy Using Image Processing and Turbulence Models. PhD Thesis, ETH-Zurich.

Förstner, W.; Gülch, E. (1987): A Fast Operator for Detection and Precise Location of Distinct Points, Corners and Centres of Circular Features. ISPRS Conference on Fast Processing of Photogrammetric Data, pp. 281-305.

Gottwald, R. (1987): Kern E2-SE – Ein neues Instrument nicht nur für die Industrievermessung? In: Allgemeine Vermessungs-Nachrichten (AVN), No. 4, pp. 147.

Harris, C.; Stephens, M. J. (1988): A Combined Corner and Edge Detector. In: Alvey Vision Conference, pp. 147-152.

Hennes, M. (1995): Entwicklung eines Messsystems zur Ermittlung von Turbulenzparametern der Atmosphäre für Anwendungen in der Geodäsie. PhD Thesis, University of Bonn.

Huep, W. (2010): Scannen mit der Trimble VX Spatial Station. In: Zeitschrift für Vermessungswesen (ZfV), No. 5, pp. 330-336.

Juretzko, M. (2006): Leistungsfähigkeit des reflektorlosen Distanzmessmoduls R300 der Tachymeterserie TPS1200 von Leica. In: Flächenmanagement und Bodenordnung, No. 68/2, pp. 90-95.

Katowski, O. (1989): Deformationsmessung an Bauwerken mit dem automatischen Theodolitmess-System ATMS. In: Proceedings of Optical 3-D Measurement Techniques, pp. 393-403.

Knoblach, S. (2011): Entwicklung, Kalibrierung und Erprobung eines kameraunterstützten Hängetachymeters. In: Allgemeine Vermessungs-Nachrichten (AVN), No. 4, pp. 122-130.

Knötzl, C.; Reiterer, A. (2010): Evaluation of an Image-Assisted Deformation Monitoring System. In: Proceedings of the Junior Scientist Conference, Vienna University of Technology.

Lanser, S.; Eckstein, W. (1992): A Modification of Deriche´s Approach to Edge Detection, In: 11th International Conference on Pattern Recognition, pp. 633-637.

Lowe, D. G. (2004): Distinctive Image Features from Scale-Invariant Keypoints. In: International Journal of Computer Vision, 2004, Vol. 60, pp. 91-110.

Marr, D.; Hildreth, E. C. (1980): Theory of Edge Detection. In: Proceedings of the Royal Society of London. No. 207, pp. 187-217.

Mosteller, F.; Tukey, J. (1977): Data Analysis and Regression. Reading, MA. Addison-Wesley.

Nakamura, J. (2006): Image Sensors and Signal Processing for Digital Still Cameras. Taylor & Francis.

Reiterer, A. (2004): A Knowledge-Based Decision System for an On-Line Videotheodolite-Based Multisensor System. PhD Thesis, Vienna University of Technology.

Reiterer, A., et al. (2009): A 3D Optical Deformation Measurement System Supported by Knowledge-Based and Learning Techniques. In: Journal of Applied Geodesy, Vol. 3, pp. 1-13.

Reiterer, A.; Huber, B.; Bauer, A. (2010): Image-Based Point Detection and Matching in a Geo-Monitoring System. In: Allgemeine Vermessungs-Nachrichten (AVN), No. 4, pp. 129-139.

Rosten, E.; Drummond, T. (2005): Fusing Points and Lines for High Performance Tracking. In: Proceedings of IEEE International Conference on Computer Vision, Vol. 2, pp. 1508-1511

Rosten, E.; Drummond, T. (2006): Machine Learning for High-Speed Corner Detection. In: Proceedings of the European Conference on Computer Vision, pp. 430-443.

Scherer, M. (2004): Intelligent Scanning with Robot-Tacheometer and Image Processing a Low Cost Alternative to 3D Laser Scanning? In: Proceedings of the FIG Working Week, Athens, Greece.

Shapiro, L. G.; Stockman, G. C. (2001): Computer Vision. Prentice Hall.

Smith, S. M.; Brady, J. M. (1997): SUSAN – A New Approach to Low Level Image Processing. In: International Journal of Computer Vision, Vol. 23, No. 1, pp. 45-78.

Steger, C. (2000): Subpixel-Precise Extraction of Lines and Edges. In: Proceedings of the XIXth ISPRS Congress, Vol.XXXIII-B3 of International Archives of Photogrammetry and Remote Sensing, pp. 141.

Steger, C. (2002): Occlusion, Clutter, and Illumination Invariant Object Recognition. In: Proceedings of the ISPRS working group III/5, Photogrammetric Computer Vision, Vol. XXXIV, Part 3A/B.

Stempfhuber, W.; Wunderlich, T. (2004): Leica System 1200: Auf dem Weg zur Sensorsynchronisation von GPS und TPS für kinematische Messaufgaben. In: Allgemeine Vermessungs-Nachrichten (AVN), No. 5, pp. 175-184.

Thuro, K. et al. (2009): Development and Testing of an Integrative 3D Early Warning System for Alpine Instable Slopes (alpEWAS). In: 17. Tagung für Ingenieurgeologie, Zittau.

Vicovac, T. (2008): Evaluierung der Leica IATS fur die konkrete Aufgabenstellung der on-line Objektrekonstruktion. Diploma Thesis, Vienna University of Technology.

Walser, B. (2004): Development and Calibration of an Image Assisted Total Station. PhD Thesis, ETH-Zürich.

Wasmeier, P. (2009): Grundlagen der Deformationsbestimmung mit Messdaten bildgebender Tachymeter. PhD Thesis, Technische Universität München.

Wolf, H. (1966): Die Beurteilung der äußeren und inneren Messgenauigkeit als ein statistisches Problem. Acta Geodaetica, Geophysica et Montanistica Acad. Sci. Hung., pp. 215-223.

WEBPAGES:

Leica Geosystems (2011): http://www.leica-geosystems.de (accessed: 12/2011).
Topcon (2011): http://www.topcon.com (accessed: 12/2011).
Trimble (2011): http://www.trimble.com (accessed: 12/2011).

AUTHORS:

Dipl.-Ing. Dr. Alexander Reiterer

CHAIR OF GEODESY
TECHNISCHE UNIVERSITÄT MÜNCHEN

Arcisstraße 21 | D-80333 München
E-Mail: alexander.reiterer@bv.tum.de

Dipl.-Ing.(FH) M.Sc. Andreas Wagner

CHAIR OF GEODESY
TECHNISCHE UNIVERSITÄT MÜNCHEN

Arcisstraße 21 | D-80333 München
E-Mail: andreas.wagner@bv.tum.de

Manuskript eingereicht: 29.07.2011 | Im Peer-Review-Verfahren begutachtet